LHAASO on Cosmic Ray Knees

Zhen Cao[1,2,3,*] *on behalf of* LHAASO Collaboration

[1]Key Laboratory of Particle Astrophyics, Institute of High Energy Physics, Chinese Academy of Sciences, 100049 Beijing, China
[2]University of Chinese Academy of Sciences, 100049 Beijing, China
[3]Tianfu Cosmic Ray Research Center, Chengdu, Sichuan, China

Abstract. LHAASO construction was complete in July 2021. The full array is operating very stably since then. All arrays, KM2A, WCDA and WFCTA are calibrated, including the absolute energy scale at 21 TeV, which was measured by using WCDA and propagated to WFCTA, with the uncertainty will be reduced down <10% in 4 years. The knee of pure proton spectrum will be measured in the first phase of the hybrid measurements of showers using four types of EAS detection techniques started in 2019 winter. Sufficient data have been collected and the analysis is in progress. Since the last run, the second phase were started in 2021 winter. The knee of the iron spectrum is the goal which will take at least 3 years of data collection. CR all-particle spectrum, composition and anisotropy are under analysis.

1 Introduction

For 110 years, Cosmic Rays (CR) have been measured for their spectrum and composition with tremendous progresses. Particularly in the last two decades, space borne spectrometers have measured spectra of individual CR species up to few hundreds of TeV with high precision based on large statistics[1][2][3][4]. New features of the spectra of CR nuclei reveal the origins and propagation in our galaxy of CRs are much more complicated than what was learned in the era in which the detection of CR composition and spectrum was limited by the precision. However, the situation has not been significantly improved in the energy range around the knee, which is still too high to the current space borne detectors. The dominant instruments are still small scale Extensive Air Shower (EAS) detector arrays with single detection techniques. Few complex EAS detection instruments with hybrid techniques are either having very high threshold energy, such as TA and PAO experiments, or at very low altitude sites, such as KASCADE, where showers at energies near the knee decayed very much, thus the measurements of EAS suffer from the shower-to-shower fluctuation. In such a way, the uncertainty in the description of the EAS development are magnified. This leads a deep entanglement between the CR composition, EAS modeling and EAS energy reconstruction. In the 30 years of development of EAS technique as a γ-ray detection technique, the high altitudes of the EAS array sites that are closer to the shower maximum depth have been found very effective in reducing the shower-to-shower fluctuation effect[5]. Multi-parameter measurements of EAS by using hybrid detection techniques eventually bring the EAS measurement in a new 'high precision' era. More conventional way of particle detection, namely identifying the primary particles before trying to reconstruct the shower energy, or multiple iteration of shower energy and composition reconstruction, eventually becomes available in EAS detection at energies around the knee. LHAASO, by taking many cutting edge techniques in the EAS detection[6], has been built and operated for this purpose. In different phases, the spectra of pure proton, pure iron nuclei, mixture of proton and helium nuclei will be measured at energies from 100 TeV to 100 PeV in years. Meanwhile, spectrum and composition of all particles will be investigated in a way that suffers less fluctuation and has huge statistics thanks to the size of the LHAASO array. In this paper, we describe the status of LHAASO as a CR detector, the multi-parameter detection, particle identification, energy reconstruction, calibration and their performances. Observational scheme for covering different energy ranges is also discussed. Some preliminary results, such as the anisotropy of CR arrival directions, and expectations are shown in the end of this paper.

2 The LHAASO Experiment

The Large High Altitude Air Shower Observatory (LHAASO) had been completely built on top of Mt. Haizi (4410 m above sea level) in the Sichuan province, China by July 2021[7]. The vertical atmospheric depth is ~600 g/cm^2. Since then, the kilometer-square array of 5216 scintillator counters and 1188 muon-detectors (KM2A) and water Cherenkov detector array (WCDA) gaplessly covering 78,000 m^2 with 3120 detector cells are fully operated with a duty cycle more than 98%. Daily rate is 2×10^8 events above 10 TeV and 3×10^9 events above 300 GeV, respectively. The wide field of view (FoV) Cherenkov telescope array (WFCTA) composing of 18 telescopes with a

*e-mail: caozh@ihep.ac.cn

5 m^2 light collector for each is also operated in dry seasons for more than 1400 hours per year. Up to now, 70 million CR events accumulated and matched with either WCDA or KM2A, thus forming a hybrid data set of CRs above 10 TeV. The shower geometry is reconstructed using the EAS arrays with very high resolutions, i.e. the shower arrival direction and the core location are measured with errors smaller than 0.2° and 3 m, respectively.

In KM2A, scintillator counters are deployed in a triangle grid with a space of 15 m between counters which is covered by a 5 mm thick lead plate, which converts secondary γ-rays into e^+e^- pairs in the counter, and measures the total deposited energy by all charged particles passing through the scintillator plates. The number of particles is measured according to the charge of single particle measured during the data taking. Muon-detectors are also in the triangle grid with a distance of 30 m between detectors, and the total active area is 40,000 m^2. With the overburden of 2.5 m soil, the muon detection has nearly zero backgrounds of e^+s, e^-s and γ-rays in a shower, except for one or two detectors very closed to the shower core. The μ-content with the threshold energy of muons ~0.9 GeV is measured for each shower. The lateral distributions of both electromagnetic particles and muons in a shower are well measured using KM2A.

In WCDA, all energy carried by e^+s, e^-s and γ-rays in a shower is deposited in water inside the detector. Cherenkov light generated in water is proportion to the deposited energy and sampled by the PMTs at the center of each cell and 4 m beneath the water surface. For showers with energy higher than 10 TeV, the lateral distribution of the energy flux is well measured as a rather smooth function. Muons in the shower could generate larger signals than electromagnetic particles since they have longer tracks in water. They could generate exceptionally large signals in cells that the muons pass through, particularly for those cells far from shower cores.

Cherenkov telescopes are operated at higher threshold energy than those of WCDA and KM2A, so events recorded by the telescopes can find their counterparts either in WCDA or/and in KM2A. With the well reconstructed shower geometry by the arrays, the images recorded by the telescopes can be used to extract a couple of shower parameters. The shower energy can be reconstructed with the total number of photons in the image by knowing exact distance between the telescope and the shower axis. Simultaneously, the angular distance between the centroid of the image and the arrival direction measures the atmospheric depth of the shower maximum as well. The shape of image has a correlation with the shower composition at certain level.

3 Detector Calibrations

The pointing calibration of the ground array KM2A and water Cherenkov detector WCDA are calibrated by measuring the standard candle, the Crab, and is found better than 0.1°[8][9]. The accurate pointing direction is essential in the hybrid measurements of showers using the EAS arrays and WFCTA.

3.1 Pointing Direction and Photometric Calibration of WFCTA

WFCTs record bright stars in their FoVs as trajectories cross over the cameras by using the integrated counting rate in 10 second of each pixel. The known directions of the stars are used to calibrate the main axes of the telescopes for their zenith angle which is measured by an inclinometers mounted on the telescope frames. The calibration accuracy is 0.023°. Within 23 days, the daily monitoring results show that the pointing errors (RMS) in zenith and azimuth angles are 0.022° and 0.029°, respectively. The minimum to maximum is less than 0.2°. Such a pointing accuracy is essential in combining the FoVs of adjacent telescopes for events that have the images cross the boundaries of individual telescopes. By including those crossing-boundary events, an enhancement of event accumulation of 30% is achieved. The images of the starts also provide perfect uniform parallel light for the calibration of the spot size for each telescope. The measured spot size with an accuracy of 3% are hard-coded in the detector simulation and the image reconstruction programms.

The photometrical calibration of telescopes has been done at two levels. The cameras are calibrated and monitored using LED sources mounted 2570 mm from faces of cameras. LEDs generate uniform surface light illuminating the cameras. The light intensity distribution across the surfaces of the cameras is measured by a photo sensor mounted on a portable 2-dimensional platform that touches to the camera surface. Absolute luminosity at each pixel is derived by the photon counts measured by a portable calibrator placed besides the cameras. The calibrator is periodically sent to National Institute of Metrology, China for calibration. Comparing the LED signals measured by pixels with nominal values, every pixel is calibrated with an overall uncertainty less than 2.6%[10]. The other level of calibration is carried out by using lasers that shoot pulses crossing the FoV of telescopes at a distance ~1 km. The light reaches the telescopes through Rayleigh scattering is calculated with a uncertainty of 7% as the known light sources. They are used to calibrate each entire telescope, including entrances, reflectors and cameras. The calibration results will be available soon.

3.2 Absolute Energy Calibration

The shadow of the Moon in galactic CRs is observed shifting westwards due to the geo-magnetic field(GMF)[11]. Given the daily updated measurements of GMF, we calculated the deflection of a mixed sample of protons and Helium nuclei according to the composition ratio measured by DAMPE[2][3] and the corresponding shift of the shadow, Δ, as a function of energies, E in TeV, of CR particles at the LHAASO site, i.e. $\Delta = 2.1^\circ/E$. Showers detected by WCDA are grouped according to the energy estimator, namely the total charge, Q recorded by the registered WCD cells in a shower event, to measure the shift of the Moon shadow, thus we have the WCDA calibrated as a shower energy detector, i.e. $E = 1.33Q^{0.95}$ GeV, where Q is in unit of number of photo-electrons. For the minimum

$\Delta = 0.06^\circ \pm 0.03^\circ$ that can be measured by WCDA which has an angular resolution of ~0.15°, the median energy is found to be 35 TeV. This is the highest calibration energy in CR experiments.

WFCTs can not be operated directly towards the Moon. The energy scale measured by WCDA is propagated to WFCTA by using commonly measured showers by the both detectors. Those showers arrive in a certain zenith window matches the FoV of the telescopes and central range of WCDA so that they are well reconstructed. The requirement of having well measured images of showers by WFCTA sets a rather high threshold above 15 TeV according to the reconstruction by WCDA which is calibrated as described above. The median energy of the group of events is (23.4±0.1) TeV. The median energy of those events reconstructed using the images measured by WFCTA is (21.9±0.1) TeV. This verifies the energy reconstruction by WFCTA with a discrepancy of 5.7%. To estimate the uncertainty of the scale itself, the event selection criteria are applied to the data set for Moon shadow measurement and the shift of the Moon shadow is measured again. It is found a shift of $0.10^\circ \pm 0.03^\circ$ of the shadow, translating to (21.0±6.5) TeV. The uncertainty of 30% is statistics dominant in the measurement of the shift. It dominates over the propagation error of 5.7% as well. The results are shown in Figure 1[12]. With time being, the statistic error of the shift measurement could reduced down below 10% in 4 years. The systematic difference between the two techniques will not longer be negligible.

4 Hybrid Measurements of Spectra of Individual CR Species

Identification of primary particle of EAS is a very challenging task. According to the experience in particle physics, measuring as many independent parameters of showers as possible is a promising way to approach. In LHAASO, four types of detectors are deployed to measure showers from different aspects, as an analog of spectrometers in collider experiments. They are the lateral distribution of shower particles (or energy flux) both at very closed region of the core within 2-3 meters and over a very extended area up to hundreds meters from the core, the content of muons and their lateral distribution over a very wide area, and the Cherenkov image of the shower development through the atmosphere. Depending on where the shower core is, at least two type of hybrid measurements of EAS are carried out in the LHAASO experiment.

One of the goals is measuring the spectra of pure proton samples and mixed proton plus helium samples (denoted as H+He) at energies around the knee, and extend the energy range down below 100 TeV where the spectra have been measured in space borne detectors such as DAMPE[2] and [3]. The knee of the proton spectrum will be unveiled with a clear transition from the spectral index from 2.7 to greater than 3.0, so that the energy range should at least start from 100 TeV and cover all energies up to 10 PeV. Showers with cores in one of the pools of WCDA of 22,500 m^2 (denoted as WCDA-1) collected in 2019-2022 observational seasons are sufficient for this purpose. This data set is also sufficient for the spectrum measurement of the H+He samples, by which a fine structure that indicates the knee of the Helium spectrum is expected to be uncovered. The coverage of higher energies might be necessary, thus larger statistics may be required. It could be achieved by having higher selection efficiency than the proton samples discussed below in detail.

The other goal is measuring the spectrum of iron around its knee at an energy that might be above 10 PeV and below the second knee around 200 PeV. This requires a much larger accumulating effective aperture for sufficient statistics at such higher energies than that for the lighter nuclei. All events with cores falling into the entire KM2A should be collected. With the spacing of 15 m between the scintillator counters, information from the shower core will be missing. For shower at such high energies, more inclined showers are selected to avoid those not having developed sufficiently so that the showers touch down the ground before reached the maxima.

For the two goals, WFCTA are configured differently and naturally divided into two phases of the observation. The first phase started with 6 telescopes deployed at the southwest corner of WCDA-1 from 2019-2020 observational season. All telescopes have the elevation angle of 60°, i.e. the zenith angle range from 22° to 38° is covered, so that there is at least 647 g/cm^2 for showers to develop in the air. Before April 2021, the hybrid operation accumulated more than 70 million events with the cores inside WCDA-1 for 720 hours during which 1/2 of KM2A were operated. The configuration of all four types of detectors is shown in Figure 2. Showers have the cores in WCDA-1, the green square area in the figure, have the most complete measurements of all parameters. The pure proton samples will be selected among them. A larger hybrid event sample can be selected with cores falling in the KM2A, e.g. the region enclosed by the red line in Figure 2. Without the parameters measured by using WCDA-1, the species identification is more difficult but it could be compensated by measuring the μ-content better because more muon detectors are registered in those showers. A mixed H+He samples could be selected among them. The large area of KM2A and higher selection efficiency than that of pure protons allow a precise measurement of the spectrum with large statistics. It is essential for searching for the fine structure of the H+He spectrum around the possible Helium knee.

In phase II starting from September 2021, all 18 telescopes are deployed to the sites near the southeast corner of WCDA-1, and form a ring-shaped FoV covering all azimuthal direction between zenith angle range from 37° to 53°. Such a setup is aiming at the detection of CRs at higher energies around the possible knee of iron spectrum, i.e. >10 PeV, so that more atmospheric depth, >751 g/cm^2, allows better developments of showers. To collect sufficient statistics,the entire KM2A needs to be used to achieve the hybrid measurements. The layout the detector arrays is illustrated in Figure 3. Since the detector configuration for the hybrid measurement of showers that have cores in WCDA-1 is very similar to Phase I, except for

more inclined, those events are also used for the pure proton analysis. This offers an important opportunity of cross checking on the proton spectrum measurements. It is also found that the events for proton showers at lower energies as those in Phase I could be also well measured at deeper atmospheric depth. It is due to the large fluctuations in shower development for protons. Showers in WCDA-1 are found measured better as well with the help of the rest part of entire WCDA in phase-II.

4.1 Multi-Parameter Analysis for Separation between Species

A typical hybrid shower event with the core inside WCDA-1 recorded in Phase-I is shown in Figure 4. In the right-upper panel, WCDA-1 measures the shower core with a huge dynamic range up to 0.2 million photoelectrons recorded in a cell as indicated by the color scale in the figure. This allows a measurement of the fine structure of the lateral distribution of the energy flux in the core. Here, shower particles have not experienced much scattering in the air so that they represent the fresh population generated not far above the surface, in other words, the hadronic components of the shower before them hit the surface. The energy flux weighted average lateral distance r_i of detector cells $< ER >= \Sigma Q_i r_i / \Sigma Q_i$, where Q_i is the charge measured by the i-th cell, is chosen as a parameter sensitive to the primary species, denoted as p_F after normalized by the preliminarily determined shower energy. The right-lower panel in Figure 4, the detection of the muon lateral distribution is shown as the number of muons in each MD. It is noticed that only handful muons recorded by each MD at distance more than 100 m from the core. Summing over all MDs between 30m and 380 m from the core for the total measured number of muons. It is a rather traditional parameter for species selection in EAS observation due to the relation $ln\mathrm{N}_\mu \sim 0.1 ln\mathrm{A}$, where N_μ is the muon content of the shower induced by a primary particle with the atomic number A. Normalized by using the total muon content in the shower, the parameter P_μ is selected as a sensitive variable for primary species identification. In the left-upper panel of Figure 4, a typical image of the shower is recorded in the camera of WFCTA. It is well known that the shower elongates longer for proton initiated shower than that by heavier nuclei. However, the length of the image depends the distance of the the shower to the telescope, R_p, due to a pure geometrical effect. Corrected by R_p and the preliminarily reconstructed shower energy, the parameter defined as the ratio of the length and the width of the image, denoted as P_C, is found sensitive to the composition of the primary species.

Before applying the multi-variate analysis to those parameters, it is important to exam the capability of the parameters individually in the primary particle identification with a simulation toolkit that takes all detector effects into account for all four type of detectors in LHAASO. In Figure 5, the distributions of the three parameters, P_F, P_C and P_μ, of proton initiated showers are plotted against the same distributions of showers initiated by Helium and all heavier nuclei. It is clear that the parameters are well selected to represent the characteristics of shower initiated by different nuclei. Here, the composition model by Gaisser *et al.*[16] is assumed. It looks a very challenging if a high purity of the proton sample, e.g. 90%, is the demand, the event selection efficiency is only ~20%. On the other hand, correlations between those parameters are found not negligible. Further efforts to find more independent parameters is still on going. Moreover, for cores falling in KM2A, P_μ and P_C are available. Selection efficiency using P_μ is even improved due to better muon content is measured than those in WCDA. Large statistics provided by the huge KM2A, makes this measurement very useful, particularly serves as cross checking.

Same parameters can be used in H+He sample selection. It is found the situation is much better than that for protons. The purity is easily to reach 95% with selection efficiency higher than 40%. Similarly, groups of independent data could cross check between the different approaches.

Finally, multivariate analysis will be applied to those data sets particularly for those have more than 3 parameters.

4.2 Energy Reconstruction

For pure proton or iron samples, the shower energy reconstruction is rather straightforward by using the total charge measured in the Cherenkov image of a shower at the impact parameter R_p from the telescope. Given the well determined shower geometry by using the EAS arrays, the shower energy uncertainty is dominated by the fluctuation of shower longitudinal development. In case of proton showers, quite symmetric resolution functions are found to be fitted with a Gaussian form with the σ to be 20% around 0.1 PeV and 15% above 1 PeV. The systematic shift of the Gaussian central expectations are less than 2% over the energy range from 0.1 to 10 PeV. The energy response function for showers at impact parameters of 120-130 m from the telescope, resolution and systematic shift as functions of shower energy and a resolution distribution at 1 PeV are shown in Figure 6. Some non-Gaussian tails are found beyond 2σ region due to the deeply developed showers were favored in the proton selection procedure. Further modification of the energy reconstruction by taking into account the EAS parameters is underdevelopment to improve the resolution.

For the mix samples with proton and Helium nuclei, the reconstruction is found more difficult due to the systematic difference as large as 7% between the two types of showers. For the hybrid samples measured by KM2A and WFCTA, the μ-content of a shower is found very helpful to compensate the difference, if a term proportional to the μ-content is included in the shower energy estimator, which was selected as the total charge of the Cherenkov image as that used for the pure proton samples. The latest progress[17] in this direction shows that the systematic difference has been reduced less than 2%.

5 All Particle Spectrum, Composition and Anisotropy Measurements

A long standing problem is that the composition, lnA, and shower energy, E, are entangled each other in CR detection using the EAS technique, if a sole shower detection technique is used in an experiment. Using the multiple EAS parameters detected by LHAASO, we are developing ways to measure the energies and the composition of the primary particles. One way is using KM2A array which measures both μ-content and the lateral distribution of shower charged particles and γ-rays, defined as EM-particles, simultaneously. For showers in the knee region, i.e. $0.1 < E < 10$ PeV, the 1 km^2 array collects sufficient statistics even only quasi-vertical events being used for the measurements. Two orthogonal linear combinations of the two densities of the EM particles and muons are found quite independent measurements of shower energy and composition[13, 14], respectively. The energy resolutions are ∼20% at 0.1 PeV and ∼10% above 10 PeV, respectively, maintaining a rather small reconstruction bias at the level below 2%. Independently, a difference of lnA at a level of ∼1 can be resolved, using the relation between average μ-content of showers induced by nuclei with atomic number A and A, i.e. $N_\mu^A = A(E/A\epsilon_c)^\beta$[15], where β is a constant index of ∼0.9 around the knee, and ϵ_c is the critical energy also a constant. The average composition is indicated by $< ln\text{A} >= (lnN_\mu^A - lnN_\mu^p)/(1-\beta)$, where the average μ-content of proton induced showers can be measured by using the pure proton samples discussed above.

The other way is using the hybrid measurements of events that detected also by WFCTA. The shower-maximum depth X_{max} is measured by using the angular difference between the direction in which the Cherenkov image has the maximum and the shower arrival direction. For showers arriving between $27^\circ < \theta < 34^\circ$ (θ is the zenith angle), the resolution is found to be ∼45 g/cm^2 for proton-like shower and ∼34 g/cm^2 for iron-like shower around 1 PeV, respectively. $< ln\text{A} >= (X_{max}^p - X_{max}^A)/k$ indicates the average composition varies with shower energy. Here, X_{max}^p and X_{max}^A are the average depths of maxima of showers induced by protons and nuclei with A nucleons. k is the *elongationrate* ∼85 g/cm^2 per decade around the knee. X_{max}^p can be measured by using the pure proton samples discussed above.

Here we see a good opportunity of cross checking between different techniques for the CR composition measurements. It is a very important investigation particularly for any possible change over the knee. Moreover, it also opens a window for a precise investigation in the PeV regime about the long standing μ-content puzzle.

The preliminary measurement of the anisotropy of CR arrival directions is done by using the KM2A data above ∼10 TeV. A clear structure with a deficit around a tenth of percent of the flux is found consistent with the 'loss cone' structure. The 'tail-in' enhancement also clearly measured at energies below 160 TeV. However, an evolution with energy of the anisotropical pattern has been revealed[18]. The corresponding systematic uncertainty has been estimated by measuring the flux variation over the period of anti-Sidereal time. It is found at least one order of magnitude lower than the signal level. Giving the huge statistics and capability of primary particle identification by KM2A, the further investigations for different species and over an even wider energy range will reveal more interesting results, particular attentions need to be on the energy dependent transition as shown in Figure 7[18].

6 Expectations and Summary

In summary, LHAASO has collected sufficient data in the hybrid measurements of charged CRs in phase-I. Both combinations by using WCDA-1 plus WFCTA and KM2A plus WFCTA are under analyzing towards producing pure proton spectrum from 100 TeV to few PeV and H+He spectrum up to 10 PeV. Sufficient number of events allows to resolve the knee of proton spectrum and fine structure around knee of Helium spectrum. The KM2A alone has also collected huge data set for all particle spectrum and composition measurements using the measurements of lateral distributions of both electromagnetic particles and μs. The hybrid data setKM2A plus WFCTA also used in the all particle spectrum and composition analyses. Many cross-checking opportunities become available for the fundamental measurements in the knee energy region. At the first time, the energy absolute calibration by measuring the 'negative beam', i.e. the Moon shadow, has been pushed to as high as 21 TeV. The operation of hybrid CR detection using the entire KM2A and WFCTA is stable with high duty cycle in phase-II, aiming at the higher energy range covering the knee of iron spectrum above 10 PeV.

Acknowledgments The author would like to thank all staff members who work at the LHAASO site above 4400 meter above the sea level year round to maintain the detector and keep the water recycling system, electricity power supply and other components of the experiment operating smoothly. We are grateful to Chengdu Management Committee of Tianfu New Area for the constant financial supports to the researches with LHAASO data. This research work is also supported by the National Key R&D program of China under the grant 2018YFA0404201.

References

[1] M. Aguilar *et al.* (AMS Coll.), Phys. Rep. **894**, 1-116, (2021).
[2] An,Q.,*et al.* (DAMPE Coll.), Science Advances, **5**, eaax3793 (2019).
[3] Alemanno, F.*et al.* (DAMPE Coll.), Phys. Rev. Lett. **126**. 201102 (2021).
[4] F. Alemanno *et al.* (DAMPE Coll.), Science Bulletin **67**, 2162, (2022).
[5] Zhen Cao, Universe **7**, 9, 339, (2021).
[6] H.H. He, Radiation Detection Technology and Methods **2**, 7 (2018).
[7] Z. Cao, Nature Astronomy **5**, 849-849 (2021).
[8] F.Aharonian, *et al.* (LHAASO Coll.), Chin.Phys. **C 45**, 025002 (2021).

[9] F.Aharonian, *et al.* (LHAASO Coll.), Chin.Phys. **C 45**, 085002 (2021).
[10] F.Aharonian, *et al.* (LHAASO Coll.), NIM, **A 1021**, 165824 (2022).
[11] A.Bartoli,*et al.* (ARGO-YBJ Coll.), Phys.Rev. **D 84**, 022003 (2011).
[12] F.Aharonian, *et al.* (LHAASO Coll.), Phys.Rev. **D 104**, 062007 (2021).
[13] Bai,L., Liu,H., on behalf of LHAASO Coll., ICRC2022, DOI: 10.22323/1.395.0246 (2022)
[14] Zhang,H., He, H., Feng, C., Phys.Rev. **D 106**, 123028 (2022).
[15] J. Matthews, Astroparticle Physics 22, 387 (2005).
[16] T. Gaisser, T. Stanev, S. Tilav, Frontiers of Physics **8**, 748 (2013).
[17] Liping Wang *et al.*, submitted to Phys.Rev. **D**, (2023).
[18] Gao,W., *et al.*, on behalf of LHAASO Coll., ICRC2022, DOI: 10.22323/1.395.0351 (2022).

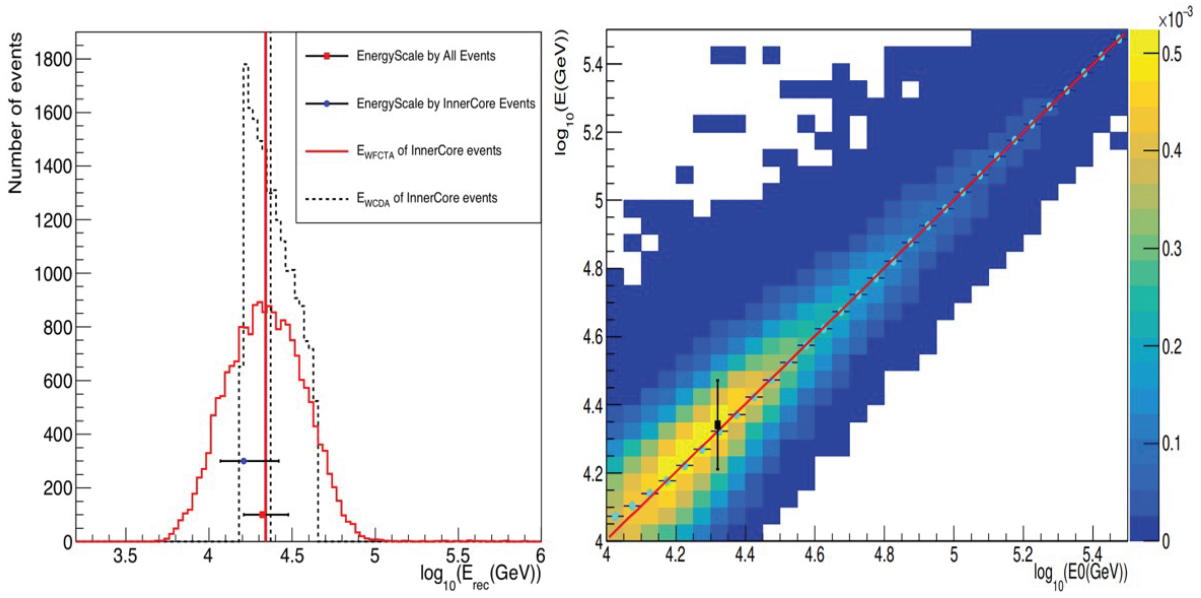

Figure 1. The energy scale measurement by WCDA (dotted histogram and the red dot with the horizontal error bar of 30% in the left panel) and propagation to WFCTA (solid histogram in the left panel). The dotted and solid vertical lines indicate the median energies[12]. The energy response function of the WFCTA is shown in the right panel. The black dot is the calibrated energy of 21.0 TeV with the 30% uncertainty shown as the error bar.

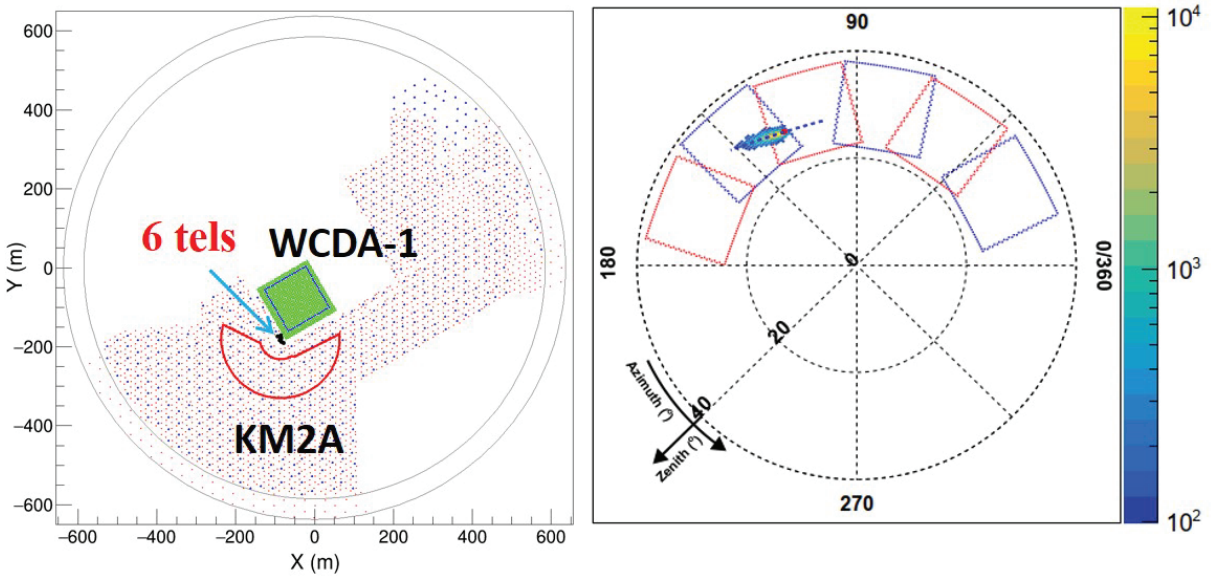

Figure 2. The configuration of LHAASO hybrid operation for cosmic ray observation before April 2021. The layout of all detectors is shown in the lefft panel. The FoV of the 6 WFCTs is shown in the right panel in the polar-coordinate system where the radius indicates the zenith angle and the polar angle in counterclockwise indicates the azimuth angle. Each square indicates the corresponding FoV of the telescope. There are overlaps between the adjacent FoV's. An image of a shower is also shown in the panel.

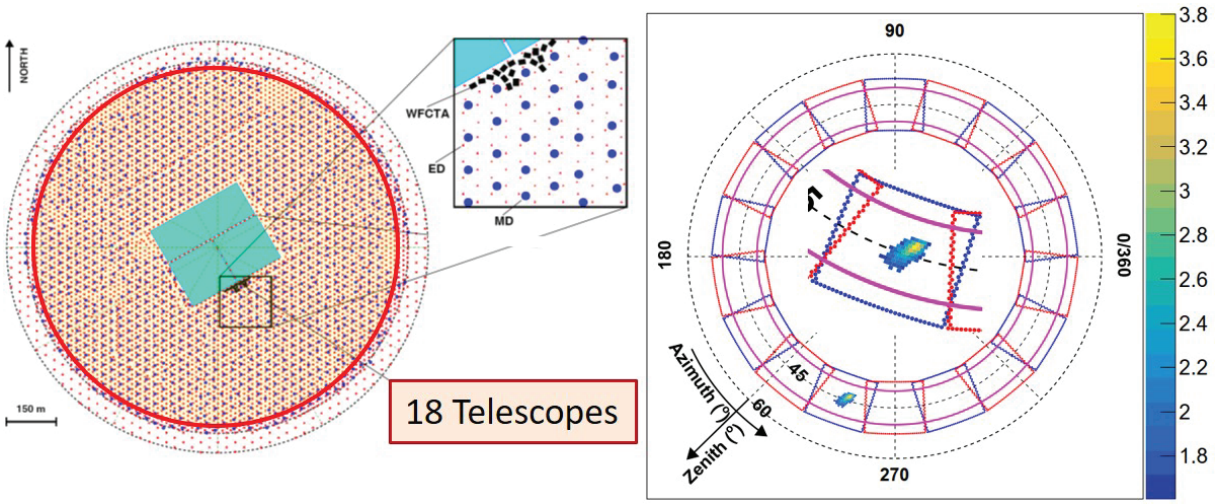

Figure 3. The configuration of LHAASO hybrid operation for cosmic ray observation after July 2021. The layout of all detectors is shown in the left panel. The FoV of the 18 WFCTs is shown in the right panel in the same coordinate system as in Figure 2. It is clearly seen that telescopes form a boundary-less FoV in the azimuthal direction between zenith angles 37° and 53°. Two zenith angle contour lines in pink indicate the event selection criteria images having heads between them, are well measured showers. The FoV of the telescope that has a shower image recorded is enlarged and put in the middle of the panel as an inset.

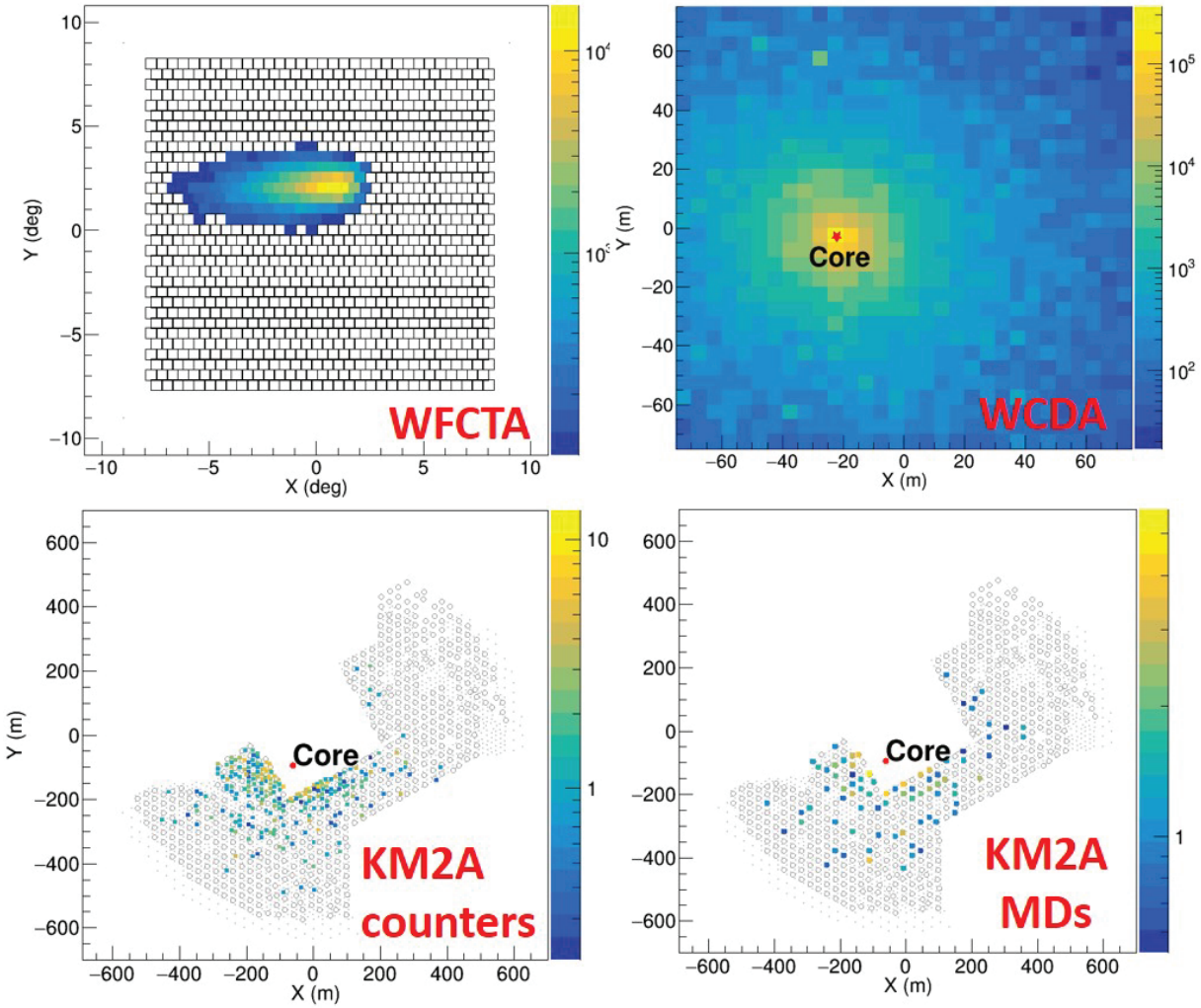

Figure 4. A typical hybrid event recorded in Phase-1.

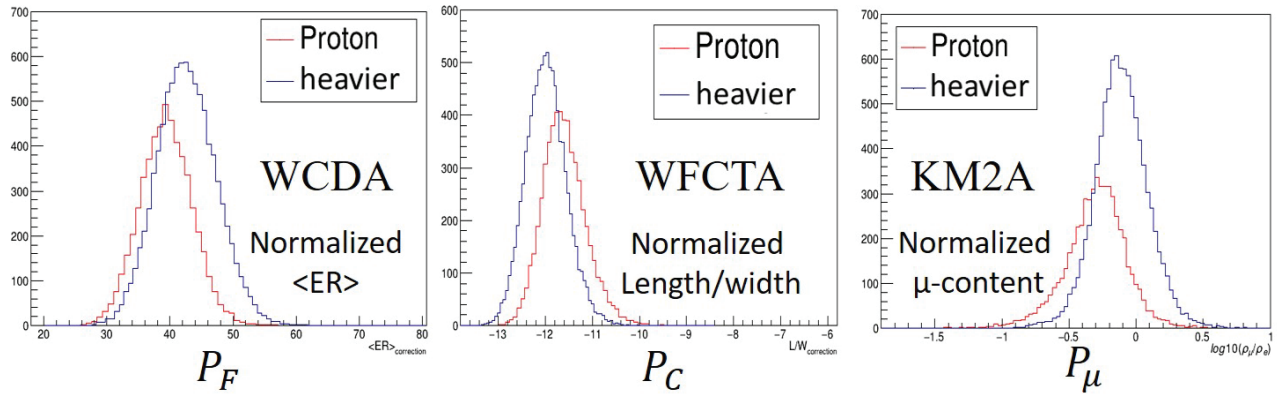

Figure 5. Primary species sensitive shower parameters measured by WCDA (P_F), WFCTA (P_C) and KM2A (P_μ), respectively. Distributions of those parameters of showers induced by protons are in red. The same distributions of showers induced by Helium and heavier nuclei are in blue, according to the composition model by Gaisser *et al.*[16].

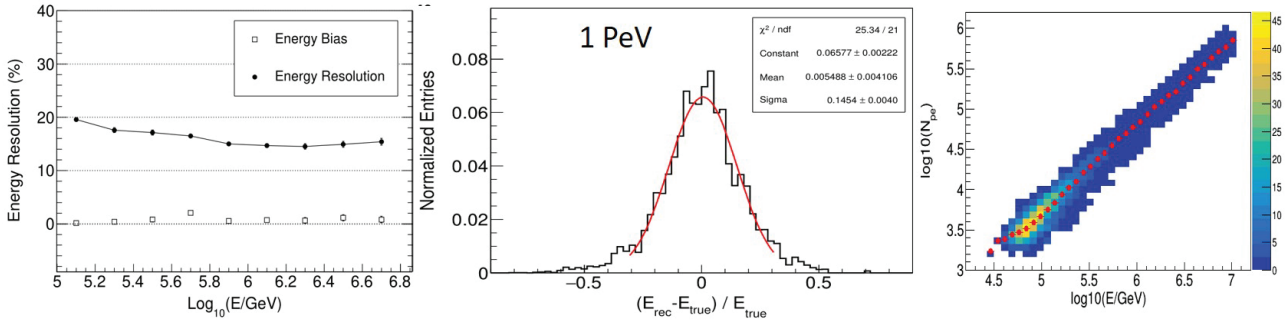

Figure 6. Energy reconstruction for pure proton samples. In the left panel, the shower energy resolution and systematic shift are shown over the energy from 100 Te V to 5 PeV. In the middle panel, the energy resolution function, i.e. the distribution of relative deviation between the reconstructed energy E_{rec} and input energy E_{true}, at 1 PeV. In the right panel, the energy response function for showers at impact parameters from 120 to 130 m from the telescope. The energy estimator is the total charge measured in the shower image in unit of number photo-electrons (N_{pe}).

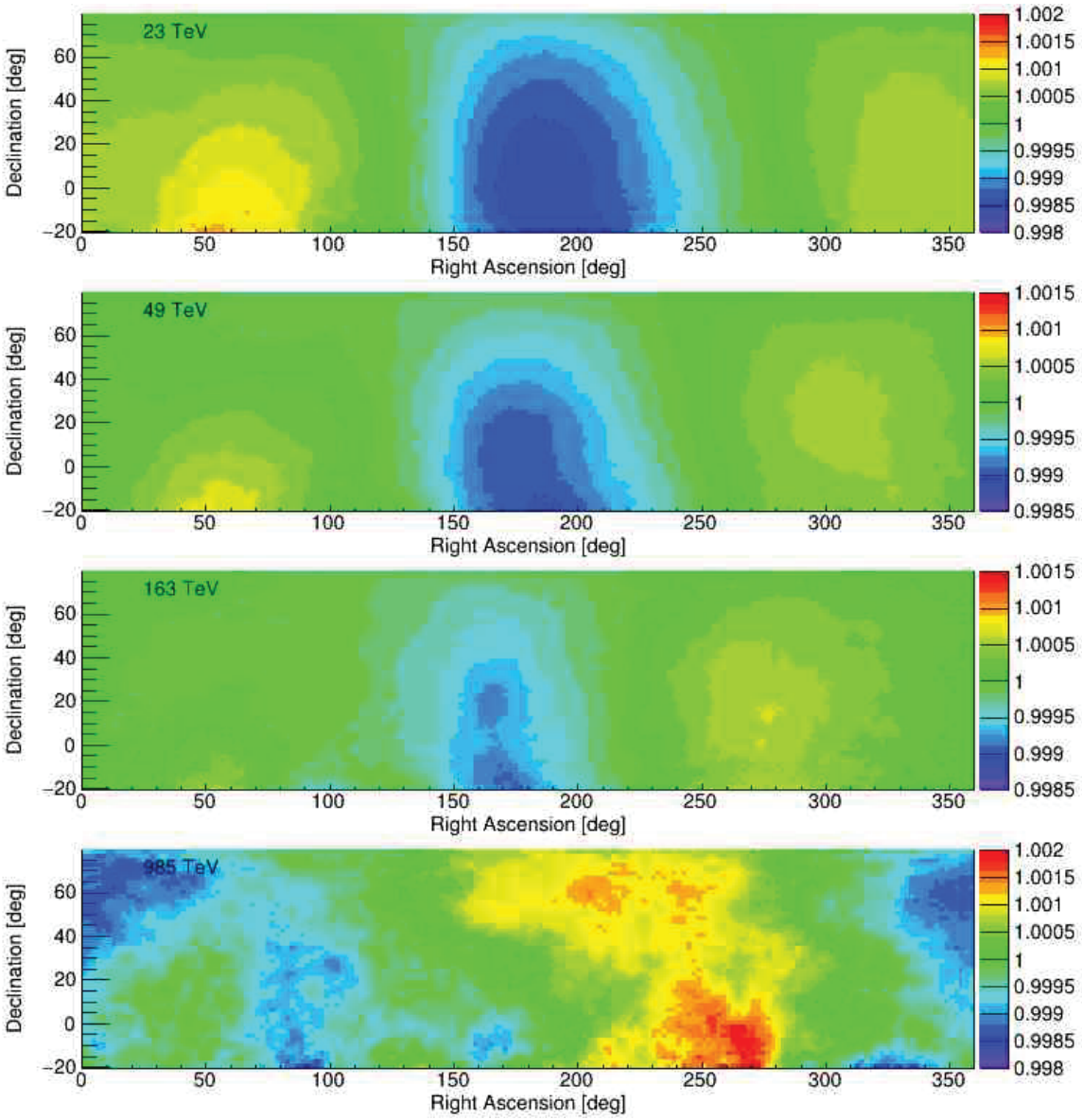

Figure 7. Anisotropy of flux of CRs at energies from 23 TeV to 1 PeV measured by KM2A[18].